Mind bomb 1 is essential for generating functional Notch ligands to activate Notch

Bon-Kyoung Koo[1,*], Hyoung-Soo Lim[1,*], Ran Song[1], Mi-Jeong Yoon[1], Ki-Jun Yoon[1], Jin-Sook Moon[1], Young-Woong Kim[1], Min-chul Kwon[1], Kyeong-Won Yoo[3], Myung-Phil Kong[1], Jinie Lee[1], Ajay B. Chitnis[2], Cheol-Hee Kim[3] and Young-Yun Kong[1,†]

[1]Division of Molecular and Life Sciences, Pohang University of Science and Technology, Pohang, Kyungbuk, 790-784, South Korea
[2]Laboratory of Molecular Genetics, NICHD, NIH, Bethesda, MD 20892, USA
[3]Department of Biology, Chungnam National University, Taejeon 305-764, South Korea
*These authors contributed equally to this work
†Author for correspondence (e-mail: ykong@postech.ac.kr)

Accepted 31 May 2005

Development 132, 3459-3470
Published by The Company of Biologists 2005
doi:10.1242/dev.01922

Summary

The Delta-Notch signaling pathway is an evolutionarily conserved intercellular signaling mechanism essential for cell fate specification. Mind bomb 1 (Mib1) has been identified as a ubiquitin ligase that promotes the endocytosis of Delta. We now report that mice lacking Mib1 die prior to embryonic day 11.5, with pan-Notch defects in somitogenesis, neurogenesis, vasculogenesis and cardiogenesis. The *Mib1*$^{-/-}$ embryos exhibit reduced expression of Notch target genes *Hes5*, *Hey1*, *Hey2* and *Heyl*, with the loss of N1icd generation. Interestingly, in the *Mib1*$^{-/-}$ mutants, Dll1 accumulated in the plasma membrane, while it was localized in the cytoplasm near the nucleus in the wild types, indicating that Mib1 is essential for the endocytosis of Notch ligand. In accordance with the pan-Notch defects in *Mib1*$^{-/-}$ embryos, Mib1 interacts with and regulates all of the Notch ligands, jagged 1 and jagged 2, as well as Dll1, Dll3 and Dll4. Our results show that Mib1 is an essential regulator, but not a potentiator, for generating functional Notch ligands to activate Notch signaling.

Key words: Notch signaling, Mind bomb, Endocytosis, Notch ligand, Mouse

Introduction

The Notch signaling pathway controls embryonic cell-fate decisions in a variety of cell lineages in flies, worms and mammals (Artavanis-Tsakonas et al., 1999). Improper Notch signaling by genetic alteration often leads to developmental defects or cancer in humans and rodents (Harper et al., 2003; Radtke et al., 2002). Thus, it is essential to identify and understand the key components of the Notch signaling pathway.

The core components in Notch signaling include the ligands Delta and Serrate, the receptor Notch, and the transcription factor Suppressor of Hairless [Su(H)] in *Drosophila*. Notch signaling is initiated by the interaction of the Notch receptor with its ligands (Lai, 2004; Schweisguth, 2004). These interactions induce proteolytic cleavage (S2) of the Notch receptors, which results in membrane-bound Notch fragments (Brou et al., 2000). After the S2 cleavage by metalloproteases, the remaining receptor fragments are cleaved at a third site (S3) within the membrane, by γ-secretase complexes containing presenilin 1 and presenilin 2, nicastrin and Aph1 (De Strooper, 2003; Mumm et al., 2000). The released intracellular fragments of Notch (Nicd) translocate to the nucleus to form transcriptional activator complexes with Su(H)/CBF1/RBP-Jκ. These complexes activate Notch target genes, such as Hairy/E(spl)-related basic helix-loop-helix (bHLH) repressors (Iso et al., 2003).

Although much is known about Notch signal transduction after the receptor undergoes the ligand-dependent S2 cleavage, the mechanism by which the Notch ligands engage Notch and trigger its cleavage is less understood. It has been proposed that the endocytosis of Notch ligands on signal-sending cells that are bound to Notch on adjacent signal-receiving cells induces the S2 and S3 cleavage of the receptor, thus activating signal transduction (Parks et al., 2000). Delta-Notch interactions result in the endocytosis of Delta in the signaling cell, which carries along the bound Notch extracellular domain, and endocytosis-defective Delta mutants have reduced signaling capacity (Parks et al., 2000). These studies in *Drosophila* suggested that the endocytosis of Notch ligands might be important for effective Notch signaling.

To date, there are two candidate genes, neuralized (Neur; Neurl in mouse) and mind bomb 1 (Mib1) that promote the ubiquitination and the endocytosis of Notch ligands. The *neur* and *mib1* mutants have defects in Notch activation in *Drosophila* and zebrafish, respectively (Boulianne et al., 1991; Itoh et al., 2003). However, disruption of the *Neur1* gene in mice did not generate the characteristic Notch phenotypes displayed by *Drosophila neur* mutants, suggesting that unknown murine Neur1 homologues might compensate for the loss of *Neur1* expression in mammals (Ruan et al., 2001; Vollrath et al., 2001). This discrepancy also raised the possibility that *Mib1* is the functional homologue of *Neur1* in

mice, because both Neur and Mib1 interact with Delta and promote its endocytosis through the ubiquitination (Le Borgne and Schweisguth, 2003).

Zebrafish *mib1* mutants exhibit not only a severe neurogenic phenotype, but also a wide range of additional defects in the development of somites, neural crest and vasculature, all indicative of defective Notch signal transduction (Jiang et al., 2000; Jiang et al., 1996; Lawson et al., 2001). The phenotypes of zebrafish *mib1* mutants are much more severe than those of *deltaA* (*dx2*), *deltaD* (*after eight*) and *notch1* (*deadly seven*) (Bingham et al., 2003; Gray et al., 2001; Riley et al., 1999). These remarkable phenotypes have suggested that *mib1* is likely to encode a core component of the Notch pathway in zebrafish. However, the lack of other zebrafish mutants with pan-Notch defects prevents a comparative study between mutants. We reported that Mib1 promotes the ubiquitination of zebrafish DeltaD and DeltaB, suggesting that Mib1 might regulate multiple ligands (Itoh et al., 2003). However, there are four Delta homologues (*deltaA*, *deltaB*, *deltaC* and *deltaD*) and three jagged (Jag) homologues (*jagged1*, *jagged2* and *jagged3*) in zebrafish. Thus, it is necessary to determine whether Mib1 regulates other ligands, such as jagged homologues and other Delta homologues, and whether Mib1 is an essential core component in Notch signaling from nematodes to mammals.

In this study, we examined whether *Mib1* plays an essential role in Notch signaling pathways by generating *Mib1*-gene targeted mice. Mib1-deficient mice exhibited pan-Notch defects, such as a lack of somitogenesis, impaired vascular remodeling and accelerated neurogenesis. Consistent with these findings, $Mib1^{-/-}$ embryos showed completely defective Notch activation, in terms of Nicd generation and Notch-target gene expression. Interestingly, Mib1 directly interacts with all of the known canonical Notch ligands [Delta-like (Dll) 1, 3 and 4, Jag1 and Jag2]. These data show that Mib1 is an essential core component of the mammalian Notch pathway that controls the function of multiple Notch ligands.

Materials and methods

Generation of *Mib1* knockout mice

The IRES-lacZ-puro cassette was fused to exon 6, with the deletion of exon 7 encoding amino acid 303 to 364 of the murine Mib1 protein (see Fig. S1A in the supplementary material). E14K ES cells were screened, and six clones showed homologous recombination. Three clones were used to generate chimeric mice after injection into C57BL/6 blastocysts. Subsequent breeding was carried out with C57BL/6 mice to generate congenic mice and with FVB/N to test the effects of the genetic background.

In situ hybridization

Details of the RNA in situ hybridizations on whole-mount or sectioned embryos were described (de la Pompa et al., 1997). Antisense DIG-labeled (digoxigenin) riboprobes were generated from pGEM-T vectors (Promega) containing amplified cDNA fragments (about 700~800 bp). Staining patterns were confirmed by comparisons with previously published data, except for *Mib1*. Probe information can be provided on request.

Histology and immunohistochemistry

For histological analysis, embryos and tissues were fixed in 4% paraformaldehyde overnight at 4°C and 4 μm sections were cut and stained with Hematoxylin and Eosin. Sections were incubated with antibodies (Abs) for Nestin (Chemicon) and huC/D (Molecular Probes) and then with Alexa-546-conjugated anti-mouse IgG Ab (Molecular Probes). For BrdU labeling, pregnant mice were injected with BrdU (150 μg/g) 2 hours before they were sacrificed. BrdU-incorporation was analyzed with an anti-BrdU FITC-conjugated Ab (BD). Apoptotic cells were detected by an in situ Cell Death Detection Kit (Roche). For Dll1 staining, 10 μm cryosections were stained with anti-Dll1 (T-20; Santa Cruz Biotechnology) Ab, followed by an Alexa-594-conjugated secondary Ab. Endothelial cell staining of whole-mount preparations was performed with a Flk1 antibody (Avas 12α1, BD) and a PECAM antibody (MEC13.3, BD), using the Vectastain Elite ABC kit (Vector Laboratories).

RT-PCR analysis

Total RNA was extracted from complete yolk sacs and embryos, using an RNeasy Micro kit (Qiagen) according to the manufacturer's instructions. Aliquots of 1 or 2 μg RNA were used for reverse transcription (Omniscript RT, Qiagen) with oligo-dT priming. Real-time RT-PCR reactions with SybrGreen quantification were set up with 1/25 of each cDNA preparation in a Roche LightCycler. Relative expression levels and statistical significance were calculated based on a β-actin standard, using the LightCycler software. All amplicons (100~200 bp) showed efficient amplification that allowed us to equate one threshold cycle difference. Primer information can be provided on request.

cDNA cloning and plasmid construction

The mouse Mib1, Dll1, Dll3, Dll4, Jag1 and Jag2 cDNAs were cloned into the pGFP-N3 (Clontech) or pCS-MT3 vectors. The ΔEN1 and Dll1 cDNAs were cloned into the *Hpa*I site of pMSCV. D. Hayward kindly provided the 8× wild-type and 8× mutant CBF Luc. All of the cDNAs amplified by PCR were sequenced and tested for expression by Western blotting.

Western blot analysis and co-immunoprecipitation assay

Embryos were homogenized in lysis buffer [10 mM Tris (pH 7.5), 150 mM NaCl, 5 M EDTA] containing a protease inhibitor mixture (Roche). Generally, 25~40 μg of protein containing supernatants were separated by size, blotted with primary and secondary Abs and visualized with ECL plus (Amersham Biosciences). The primary Abs used were as follows: rabbit anti-mouse DIP-1/Mib1 (gift from Dr Gallagher), rabbit anti-actin (Sigma), rabbit anti-mouse Hes5 (Chemicon), rabbit anti-N1icd (Cell Signaling) and mouse anti-Notch1 (mN1A; Chemicon). Immunoprecipitation was performed previously described (Koo et al., 2005).

Isolation of embryonic fibroblasts, MSCV infection, Luc assay, and neurosphere forming assay

Embryonic fibroblasts were isolated from Trypsin/EDTA digested E9.5 embryos. For MSCV virus infection, a high titer virus soup was produced with gp2-293 cells transfected with pMSCV (Clontech) and VSV-G vectors. Embryonic fibroblasts were infected for 24 hours and selected to eliminate the uninfected cells. For the CBF-Luc assay, the 8× wild-type and mutant CBF luc cassettes were transfected with pRL-TK, using Lipofectamine 2000 (Invitrogen). Luciferase activities were measured with a Dual Luciferase kit (Promega). Neurospheres were generated as described (Grandbarbe et al., 2003).

Subcellular localization analysis and flow cytometry

COS7 cells were transiently transfected with various cDNAs. Subcellular localization analysis was performed previously described (Koo et al., 2005). To detect the internalization of XD, the cells were detached with dissociation buffer (Sigma) and stained with anti-HA Ab (Santa Cruz Biotechnology) followed by anti-mouse Ab conjugated with PE (BD). All samples were analyzed by flow cytometry using a FACScan (BD).

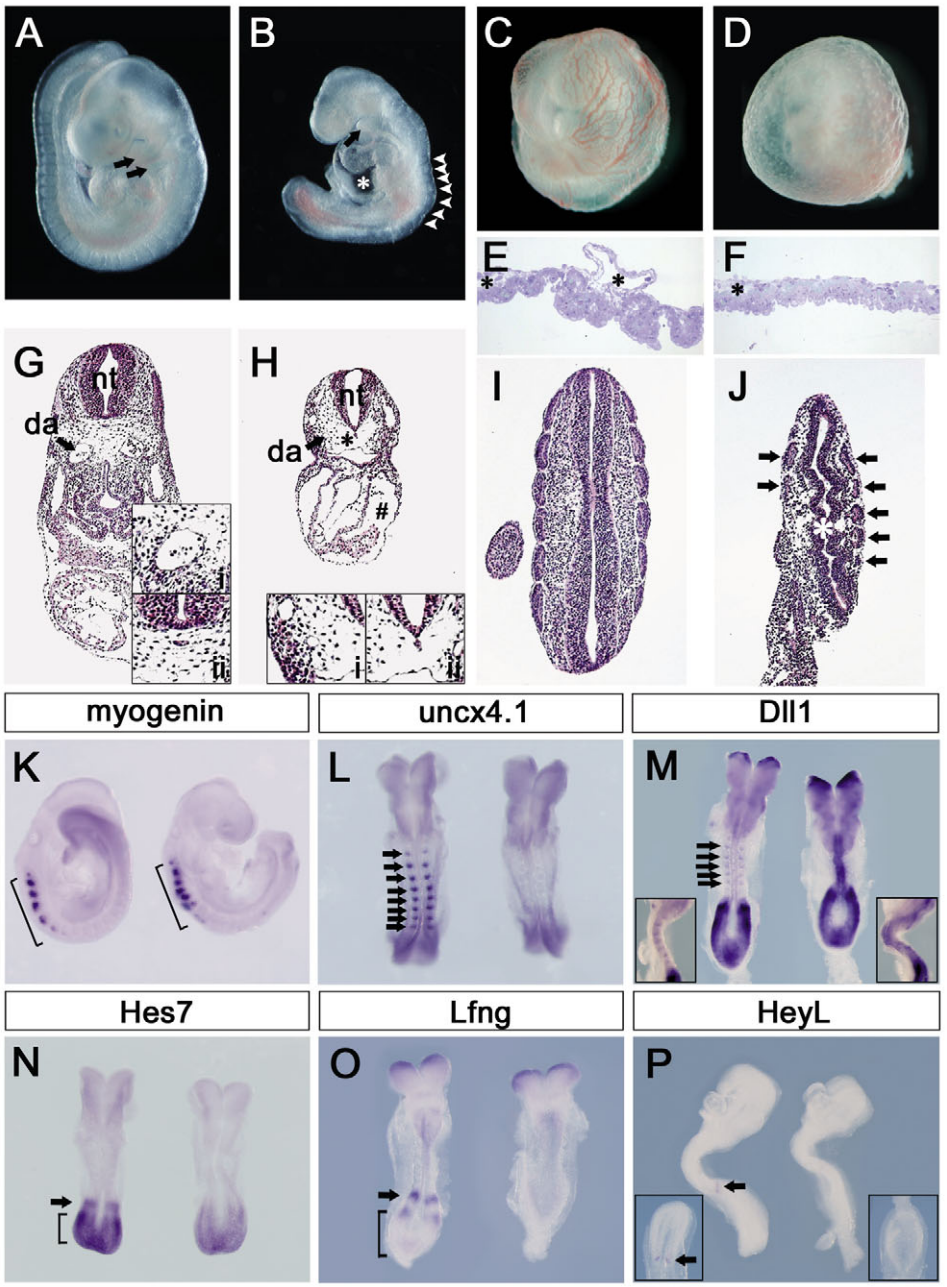

Fig. 1. Pleiotropic Notch defects in *Mib1*$^{-/-}$ embryos. (A,B) Wild-type (A) and *Mib1*$^{-/-}$ (B) embryos at E9.0. The wild-type embryo has the first and second branchial arches (A, arrows), while the *Mib1*$^{-/-}$ embryo only has the first branchial arch (B, arrow) with a distended pericardial sac (asterisk) and small, irregular somites (arrowheads). (C-F) Vascular defects in the yolk sac of E9.5 *Mib1*$^{-/-}$ embryos (D,F), as compared with the wild type (C,E). The blood vessels are indicated (asterisks). (G,H) Transverse sections of wild-type (G) and *Mib1*$^{-/-}$ (H) embryos at E9.5. The *Mib1*$^{-/-}$ embryo has a smaller dorsal aorta (da; inset i), a thinner neural tube (nt), loss of mesenchymal cells (asterisk), an enlarged pericardial cavity (#) and a fused notochord (inset ii). (I,J) Transverse section of wild-type (I) and coronal section of *Mib1*$^{-/-}$ (J) embryos at E9.5. A kinked neural tube (asterisk) and irregular somites (arrows) are evident in the *Mib1*$^{-/-}$ embryo (K) Myogenin expression (bracket) in E9.5 wild-type (left) and *Mib1*$^{-/-}$ (right) embryos. (L-P) Expression of *Uncx4.1* (L), *Dll1* (M), *Hes7* (N), lunatic fringe (*Lfng*) (O) and *Heyl* (P) in E8.5 wild-type (left) and *Mib1*$^{-/-}$ (right) embryos. The *Mib1*$^{-/-}$ embryos lack the characteristic expression of *Uncx4.1* (L, arrows), *Dll1* (M, arrows and inset), *Hes7* (M, arrow and bracket), *Lfng* (O, arrow and bracket) and *Heyl* (P, arrow and inset).

Results

Generation of *Mib1*$^{-/-}$ mice

Mib1$^{-/-}$ mice were generated as described in the supplementary material (see Figs S1, S2). At E9.5, homozygous *Mib1*$^{-/-}$ embryos were severely growth retarded, but they were present in the expected Mendelian ratio (see Table S1 in the supplementary material). *Mib1*$^{-/-}$ embryos that approximately resembled their littermates with respect to size and developmental stage could be found at E8.5, but only dead and resorbed embryos were found at E11.5-E12.5.

Pleiotropic Notch defects in embryos lacking Mib1

At E9.5, the *Mib1*$^{-/-}$ embryos always lacked blood circulation and were posteriorly truncated. Heart looping did not occur, and the *Mib1*$^{-/-}$ embryos displayed an enlarged balloon-like pericardial sac (Fig. 1B). Somitogenesis had begun albeit irregular and fused, and embryonic turning occurred in the majority of the mutants. The optic vesicles, the otic vesicles and the first branchial arches were also formed. However, the second branchial arches were completely absent (Fig. 1B). Vasculogenesis of the yolk sac was impaired in the mutants (Fig. 1D). Although an initial vascular plexus and primitive red blood cells formed, the organization into a discrete network of vitelline vessels did not occur. Furthermore, the yolk sacs had a blistered appearance. Toluidine Blue staining of semi-thin sections from wild-type and mutant yolk sacs revealed that the mutants had only small capillaries, and lacked large vitelline collecting vessels (Fig. 1F).

Transverse sections showed that the *Mib1*$^{-/-}$ embryos had smaller and thinner hearts, with broaden pericardial cavity

when compared with the wild-type embryos (Fig. 1H). These sections also revealed that the mutants had a smaller dorsal aorta, and displayed loss of mesenchyme cells and fusion of the notochord to the neural tube (Fig. 1H). These data suggest that Mib1 might be essential for somitogenesis, vasculogenesis and cardiogenesis, which are reminiscent of the Notch-related phenotypes.

Impaired somitogenesis in *Mib1*$^{-/-}$ embryos

At E8.5, the *Mib1*$^{-/-}$ embryos were of normal size and appearance, but failed to show normal somite segmentation (not shown). Transverse sections of wild-type embryos and coronal sections of *Mib1*$^{-/-}$ embryos at E9.5 also revealed unevenly divided somites, with kinked neural tubes in *Mib1*$^{-/-}$ embryos (Fig. 1I,J), while six or seven irregular somites were present in anterior region of the E9.0 wild-type and *Mib1*$^{-/-}$ embryos (Fig. 1K). To characterize the somitogenesis defects in the *Mib1*$^{-/-}$ embryos, we analyzed the expression of *Uncx4.1, Dll1*, *Hes7*, lunatic fringe (*Lfng*) and *Heyl*. The expression of *Uncx4.1*, a homeobox gene expressed in the posterior half of each somite (Leitges et al., 2000), was undetectable in the segmental plate of E8.5 *Mib1*$^{-/-}$ embryos (Fig. 1L). Consistently, the expression of *Dll1* in the posterior half of each somite was also absent (Fig. 1M). *Hes7* and *Lfng* expression normally oscillates in the presomitic mesoderm (PSM) of E8.5 wild-type embryos, but the *Hes7* expression was disturbed and *Lfng* expression was lost in the *Mib1*$^{-/-}$ embryos (Fig. 1N,O). Interestingly, the expression of *Heyl*, another Notch target gene, was completely absent (Fig. 1P). Taken together, the *Mib1*$^{-/-}$ embryos show a lack of somatic polarity and oscillation, whereas their somitic myogenesis is not altered in very early embryogenesis.

Premature neurogenesis in *Mib1*$^{-/-}$ embryos

As in zebrafish, murine *Mib1* mutants also exhibit a severe neurogenic phenotype. A histological analysis of *Mib1*$^{-/-}$ embryos isolated at E9.5 revealed localized areas of cell death, which did not seem to be random, but instead appeared preferentially in regions of the brain tissue. Picnotic cells were found in the neuroepithelium of the central nervous system, particularly in the optic lobe and the hindbrain (Fig. 2B,D,H).

At E9.0~9.5, the forebrain and hindbrain of wild-type embryos mostly consisted of nestin-positive neural precursor cells, and only a small population of cells became huC/D

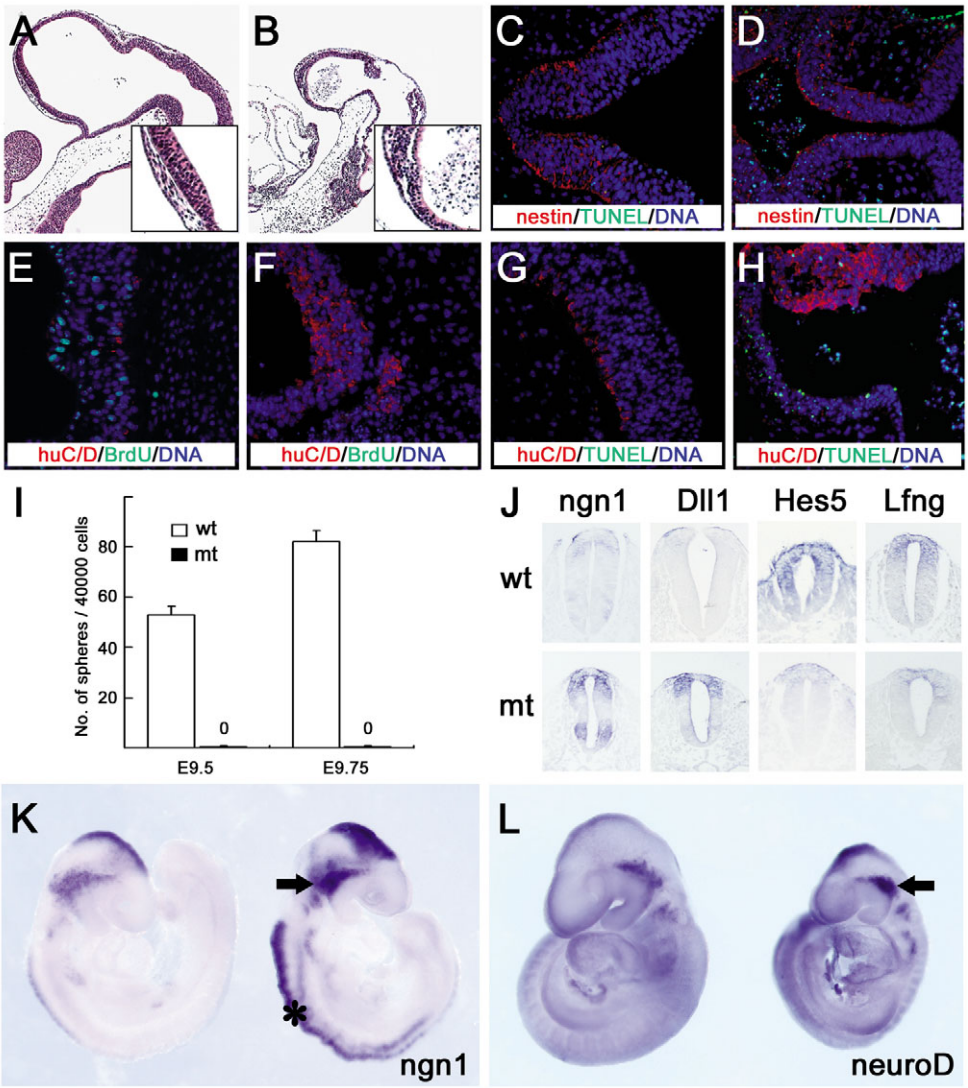

Fig. 2. Premature neurogenesis in *Mib1*$^{-/-}$ embryos. (A,B) Sagittal sections of wild-type (A) and *Mib1*$^{-/-}$ (B) embryos at E9.5. The *Mib1*$^{-/-}$ embryo has a smaller head, with picnotic cells in the brain and inside the ventricles. Enlarged views of the forebrain are shown in insets. (C-H) Sagittal and transverse sections of E9.0-E9.5 brain regions from wild-type (C,E,G) and *Mib1*$^{-/-}$ (D,F,H) embryos. Sections were stained for nestin (C,D; in red) and huC/D (E-H; in red). BrdU incorporation (E,F; in green) and TUNEL staining (C,D,G,H; in green) were used for the detection of proliferative and apoptotic cells, respectively. Nuclear DNA was stained with Hoechst (in blue). (I) Impaired neurosphere formation in *Mib1*$^{-/-}$ forebrains. Neural stem cells are absent in E9.5 (n=3) and E9.75 (n=5) *Mib1*$^{-/-}$ forebrains. (J) Expression of neurogenin 1 (*Ngn1*), *Dll1*, *Hes5* and *Lfng* in the neural tubes of E9.5 wild-type and *Mib1*$^{-/-}$ embryos. (K,L) Neurogenin 1 (*Ngn1*) (K) and *Neurod1* (L) expression in E9.5 wild-type (left) and *Mib1*$^{-/-}$ (right) embryos. Note that the expression of both *Ngn1* and *Neurod1* in the trigeminal ganglia is increased in the *Mib1*$^{-/-}$ embryos (arrows), and *Ngn1* expression is also increased in the neural tube of the *Mib1*$^{-/-}$ embryos (asterisk).

positive committed early neurons of the pial surface (Fig. 2C,E,G). By contrast, most of the brain cells in mutant embryos became huC/D positive (Fig. 2F,H). Interestingly, in spite of the massive neurogenesis, most of the cells still remained nestin positive in the mutant brains (Fig. 2D), which is similar to their phenotype in the *Hes1/5*^{DKO} mutant brain (Ohtsuka et al., 1999). In the *Mib1*$^{-/-}$ mutant brains, most of the huC/D and nestin double-positive neuronal cells might be postmitotic differentiating neurons. Consistent with the premature differentiation into immature neurons in *Mib1*$^{-/-}$ mice, the mutant brains had virtually no BrdU-positive cells, whereas the wild-type brains had proliferative zones along with the ventricle (Fig. 2E,F), indicating that the nestin-positive cells in the mutant brain were not proliferative. Moreover, the E9.5 and E9.75 *Mib1*$^{-/-}$ embryos lacked neurosphere-forming cells, suggesting the absence of a neuronal stem cell population in these stages (Fig. 2I). The mutant embryos had many TUNEL-positive cells, and large numbers of detached apoptotic cells were often visible as a mass in the ventricle (Fig. 2D,F,H).

To further examine neurogenesis in *Mib1*$^{-/-}$ embryos, we used in situ hybridization to analyze the expression of neurogenin 1 and *Neurod1*, which are bHLH transcription factors that are expressed during neuronal determination and neuronal differentiation, respectively (Ross et al., 2003). In E9.0 wild-type embryos, both neurogenin 1 and *Neurod1* were expressed mainly in the developing trigeminal ganglia (Fig. 2K,L). In E9.0 *Mib1*$^{-/-}$ embryos, neurogenin 1 was ectopically overexpressed in the neural tube, and both markers were highly induced in the trigeminal ganglia (Fig. 2K,L). To test whether the massive neurogenesis in *Mib1*$^{-/-}$ embryos is caused by a lack of Notch signaling, we examined the *Hes5* and *Lfng* expression in the neural tube. As expected, the *Mib1*$^{-/-}$ embryos lacked *Hes5* and *Lfng* expression, whereas *Dll1* expression was upregulated (Fig. 2J). Thus, Mib1 is a critical component of Notch-mediated lateral inhibition in neurogenesis (de la Pompa et al., 1997; Ma et al., 1998).

Vascular defects with the loss of arterial fate in *Mib1*$^{-/-}$ embryos

Dll4$^{-/-}$, *Notch1*$^{-/-}$ and *Hey1/2*^{DKO} mice comprise the molecular cascades for suitable arterial fate decision (Dll4→Notch1→Hey1/2) (Duarte et al., 2004; Fischer et al., 2004; Gale et al., 2004; Krebs et al., 2000; Krebs et al., 2004). We examined whether *Mib1*$^{-/-}$ embryos also have similar vascular defects, with the loss of arterial fate decision. For a detailed analysis of the vasculature, the E9.5 wild-type and *Mib1*$^{-/-}$ embryos were immunostained with an anti-Flk1 antibody to detect endothelial cells and endothelial precursors (Fig. 3A-D). The Flk1 expression revealed that vasculogenesis had occurred in both the wild-type and *Mib1*$^{-/-}$ embryos. In the *Mib1*$^{-/-}$ embryos, however, the development of the vasculature was impaired. In the head region, the vessels were thin and

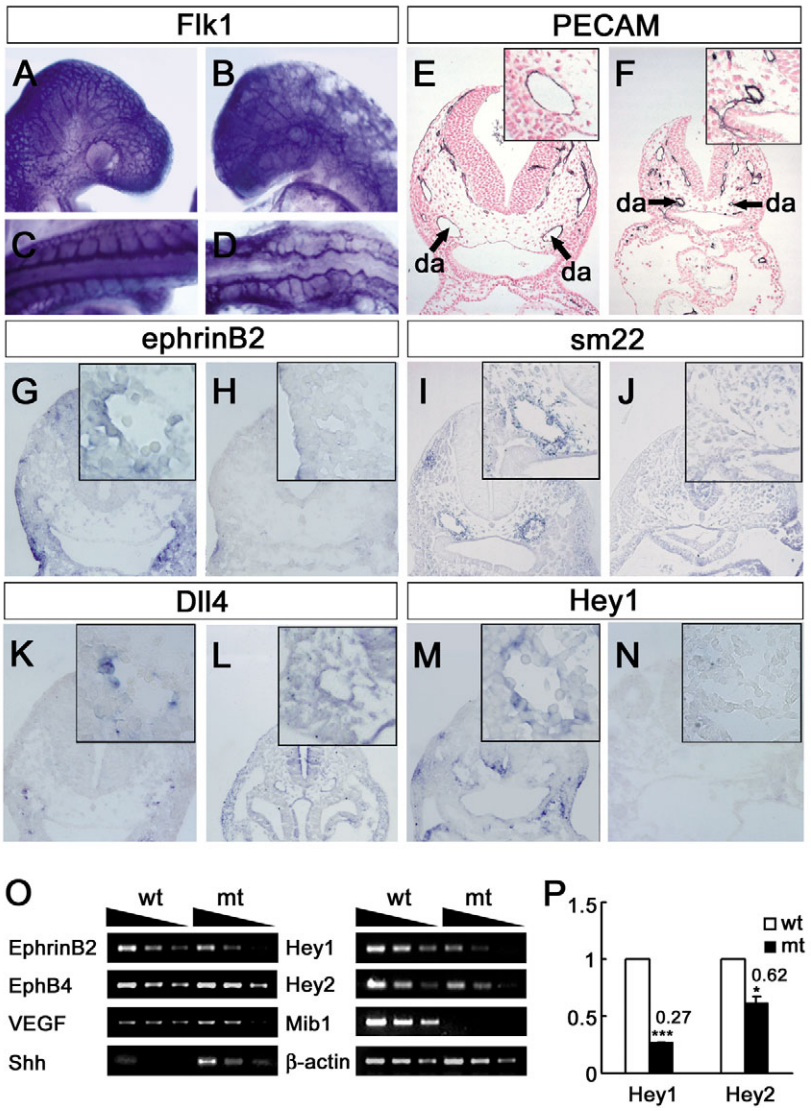

Fig. 3. Vascular defects in *Mib1*$^{-/-}$ embryos. (A-D) Whole-mount Flk1 antibody staining of E9.0 wild-type (A,C) and *Mib1*$^{-/-}$ (B,D) embryos. *Mib1*$^{-/-}$ embryos have relatively thin and disorganized blood vessels. (A,B) Lateral view of the head; (C,D) Dorsal view of the trunk. (E-N) Transverse sections of E9.0 wild-type (E,G,I,K,M) and *Mib1*$^{-/-}$ (F,H,J,L,N) embryos, stained with an anti-PECAM antibody (E,F) or labeled by in situ hybridization with specific probes for ephrin B2 (G,H), *Sm22* (I,J), *Dll4* (K,L) and *Hey1* (M,N). The PECAM-stained sections revealed the marked reduction or loss of the dorsal aorta (da) in the *Mib1*$^{-/-}$ embryos. The lack of vascular ephrin B2 expression (H; inset), smooth muscle cell recruitment (J; inset), and *Hey1* expression (N; inset) in the *Mib1*$^{-/-}$ embryos is evident, whereas the *Dll4* expression is normal (L; inset). (O,P) Expression of vascular Notch target genes (*Hey1* and *Hey2*) and genes for vasculogenesis (ephrin B2, *EphB4*, *Vegf* and *Shh*). Total RNA from E9.0 wild-type and *Mib1*$^{-/-}$yolk sacs was analyzed by semi-quantitative RT-PCR (O). The expression of *Hey1* and *Hey2* was analyzed by real-time quantitative RT-PCR (P). The numbers on each bar indicate the mean fold of induction, and the error bars indicate the standard deviation. β-actin was used for normalization. The results are representative of three independent experiments. ***P<0.0001, *P<0.01.

truncated, and did not form a finely branched tree (Fig. 3B). The intersomitic vessels that form through angiogenic sprouting were not present (Fig. 3D). This might be caused by the lack of somitic structures. However, the anterior part of the intersomitic vessels also showed an irregular ladder shape, where the somitic defects were rather mild.

To examine the defects in arterial fate decision, we analyzed the expression of PECAM, ephrin B2 (mRNA) and *sm22* (mRNA) in transverse sections of E9.0 wild-type and *Mib1*$^{-/-}$ embryos. PECAM and ephrin B2 were used as a pan-endothelial cell marker and an arterial endothelial marker, respectively (Fischer et al., 2004). *sm22* is a marker for smooth muscle cells that are recruited to the arterial endothelium (Fischer et al., 2004). All of the mutant embryos had markedly smaller dorsal aorta compared with the anterior cardinal veins (Fig. 3F). Similar to the *Dll4*$^{-/-}$, *Notch1*$^{-/-}$ and *Hey1/2*^{DKO} mutants, the *Mib1*$^{-/-}$ embryos had no or significantly reduced expression of ephrin B2 in the endothelium of the dorsal aorta (Fig. 3H) (Fischer et al., 2004). Smooth muscle cell recruitment to the dorsal aorta was also dramatically reduced, which might be caused by the loss of arterial identity (Fig. 3J).

To test whether the defect in artery formation is caused by the lack of Notch activation, we examined the expression of *Dll4* and *Hey1*, a Notch ligand and a downstream target gene for the arterial fate decision, respectively. Interestingly, *Dll4* expression was unaffected in *Mib1*$^{-/-}$ dorsal aorta, but *Hey1* expression was undetectable (Fig. 3L,N; see Fig. S3 in the supplementary material), indicating that Dll4 expression itself is not sufficient for the activation of the Notch target gene in the absence of Mib1. To further test the notion that Hey1 and Hey2 are downstream of Mib1-regulated Notch activation, RNA from the embryonic yolk sacs of E9.0 wild-type and mutant embryos was analyzed by RT-PCR and real-time quantitative RT-PCR. Both *Hey1* and *Hey2* were expressed in the wild-type yolk sacs, but the amounts of these transcripts from the *Mib1*$^{-/-}$ yolk sacs were strongly reduced, by factors of 3.7 and 1.6, respectively (Fig. 3O,P). We also detected downregulation of the arterial-specific marker ephrin B2 in the yolk sacs of *Mib1*$^{-/-}$ embryos, while the transcript level of its receptor, *Ephb4*, which is highly expressed in veins, was upregulated (Fig. 3O). Taken together, these results strongly suggest that Mib1 is an essential component involved in arterial fate decisions.

Notch signaling defects in *Mib1*$^{-/-}$ mice

Based on the multiple Notch-related phenotypes observed in *Mib1*$^{-/-}$ embryos, we tested the expression patterns of Notch-related genes. Previous studies of mutants lacking presenilin 1/2, RBP-Jκ and POFUT1 revealed the marked upregulation of *Dll1* in the neural tube and brain, with the combined loss of *Hes5* expression in the neural tube (de la Pompa et al., 1997; Donoviel et al., 1999; Shi and Stanley, 2003). In E9.0 *Mib1*$^{-/-}$ embryos, *Dll1* expression was strongly upregulated in the neural tube (Fig. 4A, part a′) with the loss of Notch target genes, such as *Hes5* and *Hey1* (Fig. 4A, parts g′,h′). Similar up- and downregulation of these genes were also detected using RT-PCR and quantitative real-time RT-PCR of E8.5 wild-type and mutant embryos (Fig. 4B,C). *Dll1* transcripts in mutant embryos were upregulated about sevenfold and Hes5 transcripts were reduced about fivefold, when compared with their wild-type counterparts. *Hes1* was downregulated in the first branchial arches (Fig. 4A, part f′). *Hey1* was also downregulated in the branchial arches and the forming somites (Fig. 4A, part h′). In situ hybridization of *Jag1* and *Lfng* in E9.0 embryos showed their reduced expression levels in the branchial arch and the PSM, respectively, of mutant embryos (Fig. 4A, parts b′,e′), while *Notch1* and *Notch2* showed comparable expression levels and patterns except in the PSM and somites (Fig. 4A, parts c′,d′). All of these results are indicative of Notch signaling defects.

To investigate the possibility that the Notch components (*Notch1*, *Notch2*, *Dll1*, *Jag1*, presenilins, mastermind 1, *RBP-Jκ* and *neur*) are defective in *Mib1*$^{-/-}$ embryos, RT-PCR analyses were performed. In short, all of these molecules were normally expressed or upregulated in E8.5 *Mib1*$^{-/-}$ embryos (Fig. 4B,C). Thus, we excluded the possibility that the *Mib1*$^{-/-}$ embryos lack essential components for Notch signaling, except *Mib1* itself.

To evaluate directly whether these remarkable changes in gene expression are caused by the lack of Notch activation, we examined the generation of the Notch1 intracellular domain (N1icd) and its target gene product, Hes5. In E9.0 wild-type whole-embryo lysates, N1icd was readily detected by western blotting. By contrast, N1icd was not observed in E9.0 *Mib1*$^{-/-}$ whole-embryo lysates (Fig. 5A). In accordance with the defective generation of N1icd, Hes5 expression was markedly reduced in *Mib1*$^{-/-}$ embryos (Fig. 5A). These defects in N1icd generation and Hes5 expression in *Mib1*$^{-/-}$ embryos were not due to the lack of Notch1 expression, as the Notch1 expression in the *Mib1*$^{-/-}$ embryos was comparable with that in the wild-type embryos (Fig. 5A). These results indicate that the *Mib1*$^{-/-}$ embryos have defects in Notch activation, especially upstream of the γ-secretase-mediated S3 cleavage.

To investigate whether the γ-secretase-mediated S3 cleavage and its downstream signaling are intact in *Mib1*$^{-/-}$ embryos, the Notch1 deleted extracellular domain (ΔEN1) was expressed in embryonic fibroblasts (EF) from wild-type and *Mib1*$^{-/-}$ embryos. ΔEN1 is readily cleaved by the γ-secretase complex to release the active N1icd, independent of a ligand/receptor interaction. In short, ΔEN1 was cleaved in both the wild-type and *Mib1*$^{-/-}$ EFs, and the cleaved N1icd was readily translocated to the nucleus to activate the transcriptional activity of downstream target genes (Fig. 5B,C,D). These results clearly show that the *Mib1*$^{-/-}$ embryos have no defect in the downstream signaling of S3 cleavage or in S3 cleavage itself. To evaluate directly the ligand function of the *Mib1*$^{-/-}$ embryos, Xdelta1-Myc (XD-Myc) was expressed in the EFs from wild-type and *Mib1*$^{-/-}$ embryos. XD-Myc-expressing EFs were co-cultured with C2C12-Notch1 cells containing CBF-Luciferase reporter gene (CBF-Luc). Notch activation was readily observed in the co-culture with XD-Myc-expressing wild-type EFs, but not in the co-culture with XD-Myc-expressing *Mib1*$^{-/-}$ cells (Fig. 5F). When the mutant CBF-Luc reporter was used, both co-cultures did not induce luciferase activity. Furthermore, when Dll1-Myc and Jag1-Myc were used instead of XD-Myc, the Notch activation was observed only in the co-culture with wild-type EFs (Fig. 5F). To test whether murine Mib1 directly induces the internalization of ligand, HA-tagged Xdelta1 (HA-XD-Myc) was co-expressed with Mib1-GFP in COS7 cells. As expected, Mib1-GFP induced internalization of Xdelta1 (Fig. 5E). Thus, the Notch signaling defects in the *Mib1*$^{-/-}$ embryos might be due to the defective endocytosis of Notch ligands.

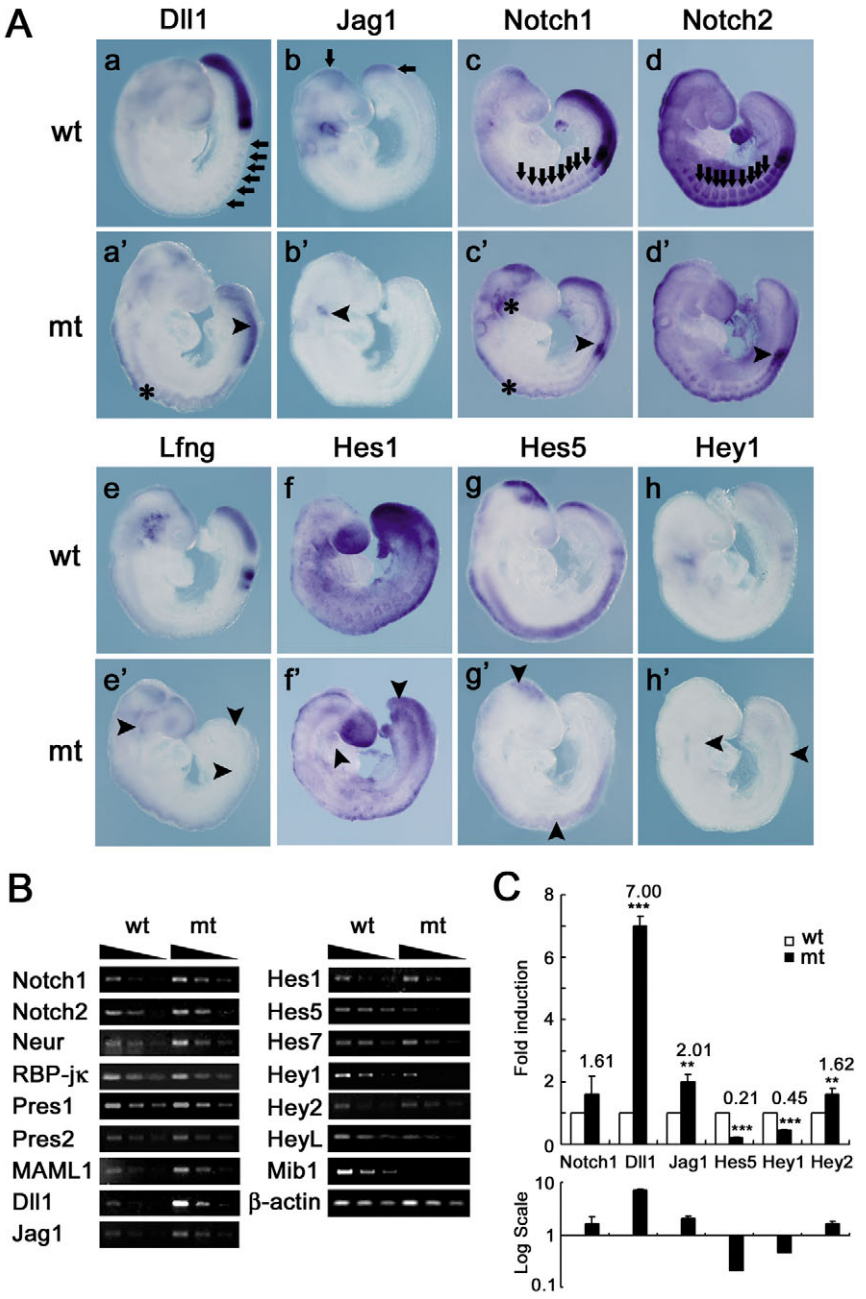

Fig. 4. Notch signaling defects in *Mib1*$^{-/-}$ embryos. (A) Lateral view of E8.75~9.0 wild-type (wt; a-h) and *Mib1*$^{-/-}$ (mt; a′-h′) embryos probed for *Dll1* (a,a′), *Jag1* (b,b′), *Notch1* (c,c′), *Notch2* (d,d′) *Lfng* (e,e′), *Hes1* (f,f′), *Hes5* (g,g′) and *Hey1* (h,h′) expression. There is ectopic overexpression of *Dll1* in the neural tube (a′; asterisk) and the downregulation of *Dll1* in the somite and PSM (a; arrows, a′; arrowhead); loss of *Jag1* expression in the head, branchial arches and presomitic region (b; arrows, b′; arrowhead); loss of *Notch1* and *Notch2* expression in somites (c,d; arrows, c′,d′; arrowheads); and ectopic overexpression of *Notch1* in the neural tube and trigeminal ganglia (c′; asterisk); the loss of *Lfng* expression in the trigeminal ganglia, newly forming somites and PSM (e′; arrowheads); and the loss of *Hes1*, *Hes5* and *Hey1* expression in the first branchial arches and PSM (*Hes1*, f′; arrowheads), the forebrain and neural tube (*Hes5*, g′; arrowheads), and the first branchial arches and newly forming somites (*Hey1*, h′; arrowheads) of the *Mib1*$^{-/-}$ embryos. (B) Expression of Notch target genes (*Hes1*, *Hes5*, *Hes7*, *Hey1*, *Hey2*, *Heyl*) and Notch pathway genes [*Notch1*, *Notch2*, *Neur*, RBP-jκ, *Pres1* (presenilin 1), *Pres2* (presenilin 2), *Maml1* (mastermind-like1), *Dll1*, *Jag1* and *Mib1*]. Total RNA from E8.5 wild-type (wt) and *Mib1*$^{-/-}$ (mt) embryos was analyzed by RT-PCR. β-actin was used for normalization. The results are representative of three independent experiments. (C) Real-time quantitative RT-PCR for *Notch1*, *Dll1*, *Jag1*, *Hes5*, *Hey1* and *Hey2*, using RNA from E8.5 wild-type (white bars) and *Mib1*$^{-/-}$ (black bars) embryos. Numbers in each bar indicate the mean fold of induction, and error bars indicate the standard deviation. ***P<0.0001, **P<0.001.

Interactions between Mib1 and all known Notch ligands

Based on molecular interactions between Mib1 and Delta, we speculated that the pan-Notch phenotypes of *Mib1*$^{-/-}$ embryos might be caused by the lack of multiple Notch ligand-mediated signaling. To test this possibility, we examined the interaction of each murine Notch ligand (three Dll and two Jag homologues) with Mib1. HA-tagged Mib1 (HA-Mib1) protein was co-immunoprecipitated with all of the Myc-tagged Delta-related Notch ligands (Dll1, Dll3 and Dll4) in HEK-293A cells (Fig. 6A). Surprisingly, Jag1 and Jag2, the Serrate-related Notch ligands, also co-immunoprecipitated with HA-Mib1 under the same conditions (Fig. 6A).

To characterize the consequences of the interactions between Notch ligands and Mib1, we tested whether murine Mib1 promotes the endocytosis of Notch ligands. Overexpression of Myc-tagged *Xenopus* Delta (XD-Myc), murine Dll1 (Dll1-Myc) and murine Jag1 (Jag1-Myc) in COS7 cells resulted in the characteristic plasma membrane expression or cytoplasmic expression with mesh-like patterns (Fig. 6B, parts b,c). When GFP-tagged Mib1 (Mib1-GFP) alone was expressed in COS7 cells, it was localized in the cytoplasm as punctate structures (Fig. 6B, part a). However, when both XD-Myc and Mib1-GFP were co-expressed, the XD-Myc expression on the cell surface was decreased, and the XD-Myc accumulated in the cytoplasm as vesicular structures where it was co-localized with Mib1-GFP, as previously described (Fig. 6B, part f) (Itoh et al., 2003). Likewise, when Dll1-Myc and Mib1-GFP (Fig. 6B, part d) or Jag1-Myc and Mib1-GFP (Fig. 6B, part e) were co-expressed in COS7 cells, the expression patterns of Dll1-Myc and Jag1-Myc were also changed, as in XD-Myc. In addition, we found the similar localization of other Notch ligands, Dll3, Dll4 and Jag2, when those ligands were co-expressed with Mib1 (data not shown).

To directly evaluate whether Mib1 regulates the endocytosis of Notch ligand in vivo, sections from E9.0 wild-type and *Mib1*$^{-/-}$ embryos were stained with anti-Dll1 antibody. The

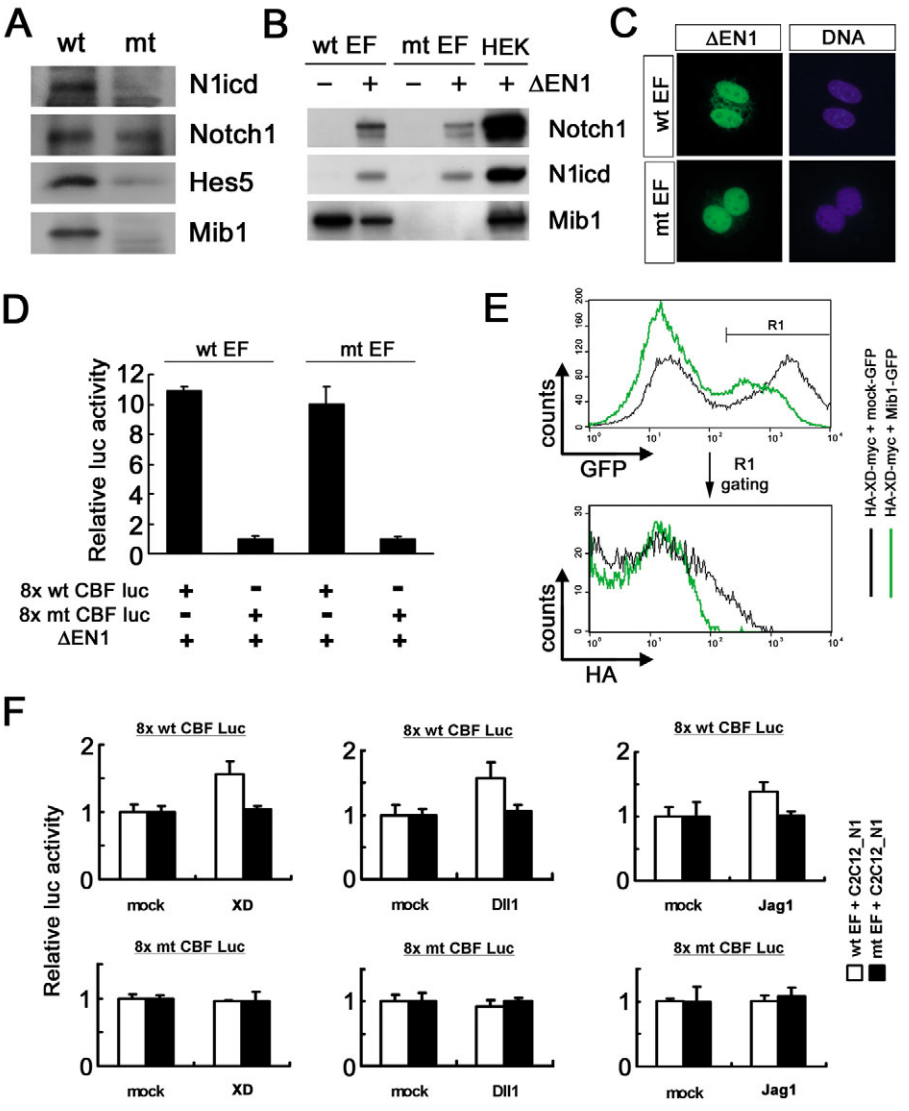

Fig. 5. Defective Notch activation in *Mib1*$^{-/-}$ embryos. (A) Notch1 intracellular domain (N1icd) generation and Hes5 expression. Lysates from E9.0 wild-type (wt) and *Mib1*$^{-/-}$ (mt) embryos were immunoblotted with rabbit anti-N1icd, mouse anti-Notch1, rabbit anti-mouse Hes5 and rabbit anti-Mib1 antibodies. The results are representative of three independent experiments. (B-D) S3 cleavage of Notch1 by γ-secretase. Embryonic fibroblasts (EFs) isolated from E9.5 wild-type (wt) and *Mib1*$^{-/-}$ (mt) embryos were infected with the MSCV vector driving the expression of Myc-tagged extracellular domain-deleted Notch1 (ΔEN1). (B) Western blot analysis of Nicd generation. Cell lysates were immunoblotted with anti-Notch1, anti-N1icd and anti-Mib1 antibodies. HEK293A cells (HEK) were used as a positive control for infection and N1icd generation. There is intact N1icd generation in *Mib1*$^{-/-}$ EFs. (C) Nuclear transport of Nicd. Infected cells were fixed and immunostained with an anti-Myc antibody, followed by anti-mouse Alexa-488 (in green). Nuclear DNA was stained with Hoechst (in blue). N1icd are transported intra-nuclearly in *Mib1*$^{-/-}$ EFs. (D) CBF-luciferase (Luc) activation by Nicd. The 8× wild-type and mutant CBF-Luc vectors were transfected to measure the activity of N1icd in MSCV_ΔEN1-infected wild-type and *Mib1*$^{-/-}$ EFs. The 8× mutant CBF-Luc lacks the CBF-binding sites and was used as a control. The relative Luc activities of wild-type and *Mib1*$^{-/-}$ EFs are comparable. (E) Internalization of Delta by murine Mib1. COS7 cells were transfected with either mock GFP or HA and Myc-tagged *Xenopus* Delta (HA-XD-Myc) (black) or Mib1-GFP and HA-XD-Myc (green). Twenty-four hours after transfection, the cells were stained with anti-HA Ab followed by PE-conjugated anti-mouse Ab and analyzed by flow cytometry. (F) Defective Notch signaling in the *Mib1*$^{-/-}$ EFs. The wild-type (white bar) and *Mib1*$^{-/-}$ (black bar) EFs infected with MSCV vector driving the expression of Myc-tagged *Xenopus* Delta (XD), Myc-tagged mouse Delta1 (Dll1) or Myc-tagged mouse jagged 1 (Jag1) were co-cultured with C2C12-Notch1 cells transfected with the 8× wild-type and mutant CBF-Luc vectors. Twenty-four hours after co-culture, luciferase activity was measured. The 8× mutant CBF Luc was used as a control for Notch activation.

Dll1 in wild-type embryos was localized in the cytoplasm near the nucleus (Fig. 6C). Surprisingly, in *Mib1*$^{-/-}$ embryos, Dll1 exclusively accumulated in the plasma membrane (Fig. 6C). All of these observations indicate that murine Mib1 is essential for the endocytosis of Notch ligand.

Discussion

In large-scale mutagenesis screens, zebrafish *Mib1* mutants were initially identified by their neurogenic phenotype, which is a hallmark for the disruption of Notch signaling (Jiang et al., 1996; Schier et al., 1996). Recently, Mib1 has been identified as an E3 ubiquitin ligase that interacts with Delta to promote its ubiquitination and internalization, and to potentiate its signaling activity in the signal-sending cells (Itoh et al., 2003). As the overexpression of *Xdelta* in zebrafish *Mib1* mutants rescues the neurogenic defect, it has been suggested to be a potentiator in generating functional Delta ligands to activate Notch (Itoh et al., 2003). However, by generating *Mib1*$^{-/-}$ mice, we have clearly demonstrated that Mib1 is an essential regulator of Notch ligand activation, but not a potentiator, and this ligand activation is absolutely required for Notch signaling.

The *Mib1*$^{-/-}$ mice exhibit multiple Notch-related phenotypes, such as defects in somitogenesis, neurogenesis, vasculogenesis and cardiogenesis. In addition, the *Mib1*$^{-/-}$ embryos showed an enlarged balloon-like pericardial sac, fusion of the notochord to the neural tube, disorganization of the trunk ventral neural tube, loss of mesenchyme cells, and abnormal heart and second branchial arch development. The phenotypes of the *Mib1*$^{-/-}$ embryos most closely resemble those of embryos that lack core Notch signaling components, such as Pofut, presenilins 1/2 and RBP-Jκ (de la Pompa et al., 1997; Donoviel et al., 1999; Oka et al., 1995; Shi and Stanley,

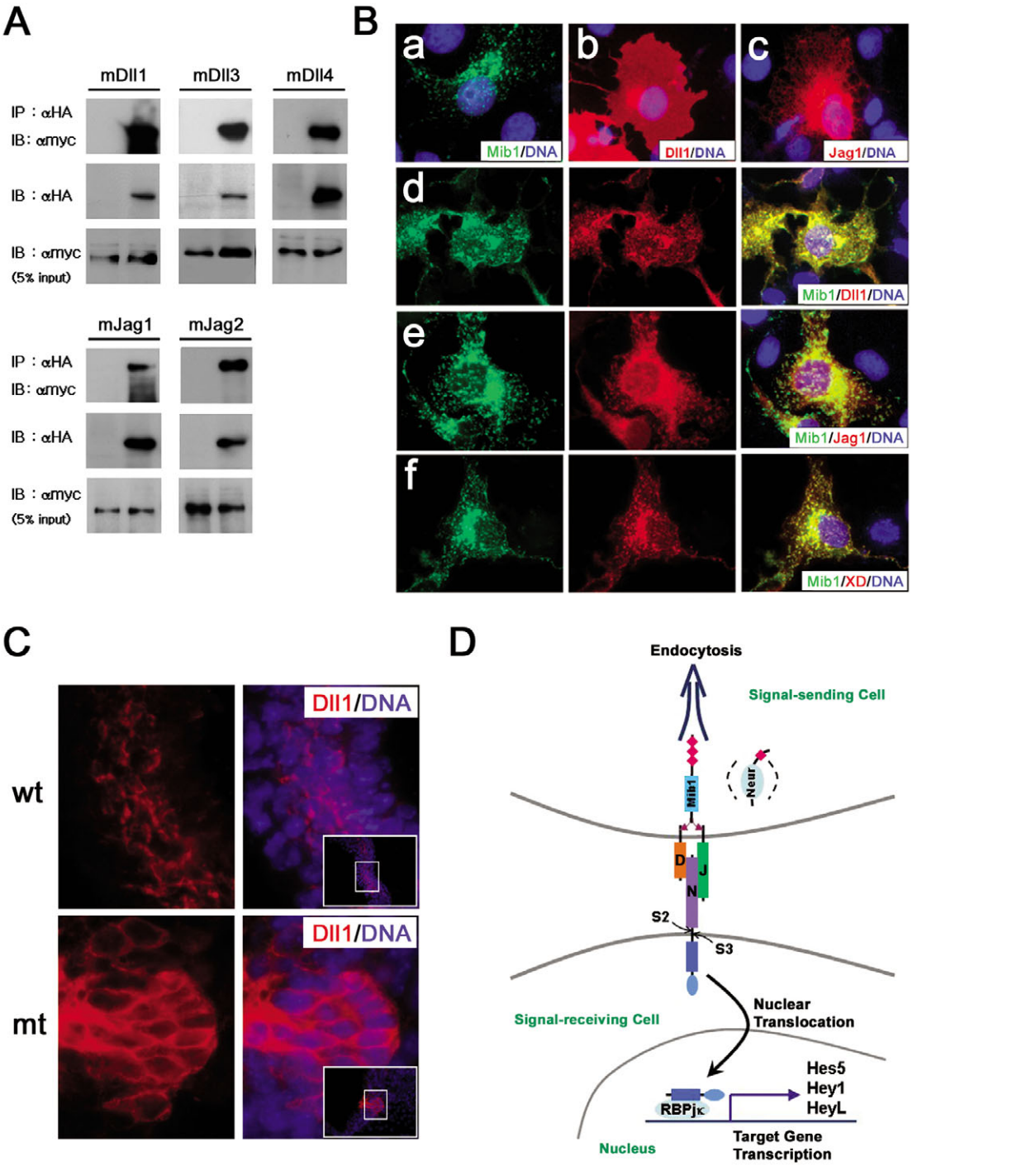

Fig. 6. Interactions between Mib1 and all known Notch ligands. (A) Co-immunoprecipitation (Co-IP) of murine Mib1 with murine Notch ligands (Dll1, Dll3, Dll4, Jag1 and Jag2). HA-tagged Mib1 (HA-Mib1) or control vectors were co-expressed with Myc-tagged Notch ligands in HEK293A cells. The top panels show IP of Notch ligands by HA-Mib1, and the middle and bottom panels show the expression of HA-Mib1 and Notch ligand-Myc, respectively, in total cell lysates. (B) Subcellular localization of Mib1 (in green) and Notch ligands (Dll1, Jag1 and XD; in red). Mib1-GFP and/or Myc-tagged Notch ligand constructs were co-expressed in COS7 cells. Myc epitopes were detected with an anti-Myc antibody followed by a TRITC-labeled antibody. Nuclear DNA was stained with Hoechst (in blue). (a-c) Expression of Mib1-GFP (a), Dll1-Myc (b) and Jag1-Myc (c). (d-f) Co-transfection of Mib1-GFP with either Dll1-Myc (d), Jag1-Myc (e) or XD-Myc (f). Overlapping expression is yellow. (C) Transverse sections of E9.0 wild-type (wt) and *Mib1*$^{-/-}$ (mt) embryos stained with anti-Dll1 antibody. Dll1 is localized in the cytoplasm in wild-type neural tube, and accumulates in the plasma membrane in *Mib1*$^{-/-}$ neural tube (in red). Nuclear DNA was stained with Hoechst (in blue). The overall images are shown in insets. (D) Notch signal transduction. The pan-Notch phenotype in *Mib1*$^{-/-}$ embryos and the molecular interactions between Mib1 and multiple Notch ligands suggest a new core-Notch component that regulates the endocytosis of Dll and Jag ligands. The endocytosis of the Notch ligands by Mib1 stimulates the S2 and S3 cleavages of Notch receptors and the released Nicd translocates to the nucleus to express the Notch target genes, such as Hes5, Hey1 and Heyl.

2003). In accordance with the pan-Notch defects in *Mib1*$^{-/-}$ embryos, expression of the Notch target genes, such as *Hes5*, *Hey1* and *Heyl*, was dramatically downregulated. In neurogenesis, the *Mib1*$^{-/-}$ embryos exhibited the characteristic loss of Hes5 expression in the neural tube and premature neuronal differentiation accompanied by the depletion of neural stem cells (de la Pompa et al., 1997; Donoviel et al., 1999). In somitogenesis, the *Mib1*$^{-/-}$ embryos showed the loss of Uncx4.1 expression and defects in *Hes7* and *Lfng* oscillation (Barrantes et al., 1999). Moreover, the *Mib1*$^{-/-}$ embryos displayed the loss of ephrin B2 and *Hey1* expression in the dorsal aorta (Krebs et al., 2004). These results are all indicative of a lack of Notch activation and are characteristic pan-Notch phenotypes in mutants lacking core Notch signaling components, such as Pofut, presenilins 1/2 and RBP-Jκ. In addition to the downregulation of Notch target gene expression, the *Mib1*$^{-/-}$ embryos also showed a complete loss of N1icd generation, despite the normal expression of core components for Notch signaling, such as presenilins, Notch proteins and Notch ligands.

There are five canonical Notch ligands (Dll1, Dll3, Dll4, Jag1 and Jag2) in mammals (Lai, 2004). A previous study revealed that Mib1 directly regulates the endocytosis of zebrafish DeltaB and DeltaD (Itoh et al., 2003). However, the endocytosis of Serrate-related ligands by E3 ubiquitin ligases has not been investigated, although it has been shown that Serrate, like Delta, is a transmembrane ligand that can participate in the trans-endocytosis of Notch to the ligand expressing cells (Klueg and Muskavitch, 1999). Each Notch ligand has redundant and non-redundant roles in the Notch activation pathway at various cell fate decisions. Dll1 and Dll3 are required for the proper anteroposterior polarity of each somite (Barrantes et al., 1999; Hrabe de Angelis et al., 1997; Kusumi et al., 1998). Dll4 is crucial in the arterial fate decision (Duarte et al., 2004; Gale et al., 2004; Krebs et al., 2004). Jag1 and Jag2 are essential for remodeling of the embryonic vasculature, and for limb and craniofacial development, respectively (Jiang et al., 1998; Xue et al., 1999). The pan-Notch phenotypes in *Mib1*$^{-/-}$ embryos could be explained by the combined loss of multiple ligands. The defects in somitogenesis, the loss of *Uncx4.1* and *Heyl* expression, and the impaired oscillations of *Hes7* and *Lfng* can be explained by the combined loss of Dll1 and Dll3. The defects in vasculogenesis and the loss of *Hey1* and ephrin B2 expression closely resemble the vascular phenotypes in *Dll4*$^{-/-}$ mice. Although the *Mib1*$^{-/-}$ embryos do not clearly explain the phenotypes in *Jag1*$^{-/-}$ and *Jag2*$^{-/-}$ mice, the thin vascular network and the defect in the second branchial arch development appear to represent the loss of Jag1 and Jag2 activity, respectively. In accordance with the pan-Notch phenotypes in *Mib1*$^{-/-}$ embryos, Mib1 interacts with all of the Notch ligands, Jag1 and Jag2 as well as Dll1, Dll3 and Dll4, and induces their endocytosis, suggesting that all of these defects might be due to the inactivation of most, if not all, of the Notch ligand functions.

A crucial step for efficient Notch signaling by Delta was revealed by an analysis of *Drosophila neur* and zebrafish *Mib1* mutants (Deblandre et al., 2001; Itoh et al., 2003; Lai et al., 2001; Pavlopoulos et al., 2001). These two genes promote the endocytosis of Delta in a ubiquitination-dependent manner. It has been proposed that the endocytosis of Notch ligands, on signal-sending cells that are bound to Notch on adjacent signal-receiving cells, induces the S2 cleavage of the receptor, thus activating signal transduction (Parks et al., 2000). Surprisingly, in *Mib1*$^{-/-}$ mutants, the expression of Dll1 was accumulated in the plasma membrane, while it was localized in the cytoplasm near the nucleus in the wild type, indicating that Mib1 is essential for the endocytosis of Dll1. Consistent with the endocytic defects of Notch ligand, Notch activation, such as the generation of Nicd and the activation of Notch-target genes, was abolished. Thus, our data clearly show that Mib1 is an essential regulator of Notch ligand endocytosis and activation of Notch signaling.

Although both Neur and Mib1 interact with Delta and regulate its endocytosis, it is not clear whether they have redundant or unique, non-redundant functions in Notch signaling. Consistent with previous studies in zebrafish *Mib1* mutants, our *Mib1*$^{-/-}$ mice exhibited pan-Notch defects, indicating that Mib1 has non-redundant roles in Notch signaling in both zebrafish and mammals. Most recently, two groups have reported the serrate-related function of *Drosophila Mib1* and they also showed replaceable function of *Drosophila* Mib1 and *Drosophila* Neur (Lai et al., 2005; Le Borgne et al., 2005). In contrast to our *Mib1*$^{-/-}$ mice exhibiting pan-Notch defects, *Drosophila Mib1* mutants display part of the Notch phenotypes, suggesting functional redundancy between *Drosophila* Mib1 and *Drosophila* Neur. In our recent study, we identified a Mib1 paralogue, Mib2, which has similar activities, but different expression patterns compared with those of Mib1 (Koo et al., 2005). *Mib2* is mainly expressed in the adult tissues, but not in early embryonic stages, whereas *Mib1* is abundantly expressed in both embryos and adult tissues, suggesting *Mib1* might have a dominant role during early embryogenesis. However, it is not tested whether *Drosophila mib2* (CG17492) has an essential or redundant role in the *Drosophila* Notch signaling pathway. *neur* mutants in *Drosophila* are characterized by neurogenic phenotypes and have defects in Notch activation (Boulianne et al., 1991; Price et al., 1993). However, the disruption of the *Neur* gene in mice did not generate the characteristic Notch phenotypes as in *Drosophila neur* mutants (Ruan et al., 2001; Vollrath et al., 2001). This discrepancy suggests that unknown murine *neur* homologues and/or murine *Mib1* can compensate for the loss of *Neur* in mammals. There are two murine neuralized genes, *Neur1* and *Neur2,* which have similar phylogenic distances from *Drosophila neur* (R.S. and Y.-Y.K., unpublished), suggesting that double mutants of murine *Neur1* and *Neur2* might have defects equivalent to those observed in *Drosophila neur* mutants. Considering the evolutionary conservation of the Notch signaling pathway, it will be interesting to examine whether these two regulators, *Neur* and *Mib1*, play cooperative but non-redundant roles in mammals.

Mib1 has been suggested to be a potentiator in generating functional ligands because of the residual Notch activity in zebrafish *Mib1* mutants (Cheng et al., 2004; Itoh et al., 2003). The ectopic overexpression of *Xdelta* rescues the neurogenic defect in zebrafish *Mib1* mutants and Notch activation was further suppressed by expression of dominant-negative Su(H). By contrast, we have identified Mib1 as an essential regulator in generating functional Notch ligands (Fig. 6D). This discrepancy might be due to the effects of maternal genes as *Mib1* transcripts are expressed maternally in zebrafish

unfertilized eggs (Itoh et al., 2003). Furthermore, Mib1 interacts with all of the murine Notch ligands, and genetic inactivation of Mib1 results in multiple developmental defects that are characteristic of impaired Notch signaling. Thus, our data provide the first evidence in mammals that the E3 ubiquitin ligase Mib1 is an essential core component of Notch signaling.

Supplementary material

Supplementary material for this article is available at
http://dev.biologists.org/cgi/content/full/132/15/3459/DC1

We thank D. S. Lim and J. K. Han for helpful comments, P. J. Gallagher for the DIP-1 antibody, D. Hayward for the 8× wild-type and mutant CBF-Luc, G. Weinmaster for the C2C12-Notch1 cell line, and J. M. Penninger for critical reading of the manuscript. This work was supported by grants from the Vascular System Research Center from KOSEF, Basic Research Program of the Korea Science and Engineering Foundation (R02-2003-000-10057-0), the 21C Frontier Functional Human Genome Project from Ministry of Science and Technology of Korea (FG04-22-05), and the Molecular and Cellular BioDiscovery Research Program grant from the Ministry of Science and Technology, South Korea (M1-0106-01-0001).

References

Artavanis-Tsakonas, S., Rand, M. D. and Lake, R. J. (1999). Notch signaling: cell fate control and signal integration in development. *Science* **284**, 770-776.

Barrantes, I. B., Elia, A. J., Wunsch, K., Hrabe de Angelis, M. H., Mak, T. W., Rossant, J., Conlon, R. A., Gossler, A. and de la Pompa, J. L. (1999). Interaction between Notch signalling and Lunatic fringe during somite boundary formation in the mouse. *Curr. Biol.* **9**, 470-480.

Bingham, S., Chaudhari, S., Vanderlaan, G., Itoh, M., Chitnis, A. and Chandrasekhar, A. (2003). Neurogenic phenotype of mind bomb mutants leads to severe patterning defects in the zebrafish hindbrain. *Dev. Dyn.* **228**, 451-463.

Boulianne, G. L., de la Concha, A., Campos-Ortega, J. A., Jan, L. Y. and Jan, Y. N. (1991). The Drosophila neurogenic gene neuralized encodes a novel protein and is expressed in precursors of larval and adult neurons. *EMBO J.* **10**, 2975-2983.

Brou, C., Logeat, F., Gupta, N., Bessia, C., LeBail, O., Doedens, J. R., Cumano, A., Roux, P., Black, R. A. and Israel, A. (2000). A novel proteolytic cleavage involved in Notch signaling: the role of the disintegrin-metalloprotease TACE. *Mol. Cell* **5**, 207-216.

Cheng, Y. C., Amoyel, M., Qiu, X., Jiang, Y. J., Xu, Q. and Wilkinson, D. G. (2004). Notch activation regulates the segregation and differentiation of rhombomere boundary cells in the zebrafish hindbrain. *Dev. Cell* **6**, 539-550.

de la Pompa, J. L., Wakeham, A., Correia, K. M., Samper, E., Brown, S., Aguilera, R. J., Nakano, T., Honjo, T., Mak, T. W., Rossant, J. et al. (1997). Conservation of the Notch signalling pathway in mammalian neurogenesis. *Development* **124**, 1139-1148.

De Strooper, B. (2003). Aph-1, Pen-2, and Nicastrin with Presenilin generate an active gamma-Secretase complex. *Neuron* **38**, 9-12.

Deblandre, G. A., Lai, E. C. and Kintner, C. (2001). Xenopus neuralized is a ubiquitin ligase that interacts with XDelta1 and regulates Notch signaling. *Dev. Cell* **1**, 795-806.

Donoviel, D. B., Hadjantonakis, A. K., Ikeda, M., Zheng, H., Hyslop, P. S. and Bernstein, A. (1999). Mice lacking both presenilin genes exhibit early embryonic patterning defects. *Genes Dev.* **13**, 2801-2810.

Duarte, A., Hirashima, M., Benedito, R., Trindade, A., Diniz, P., Bekman, E., Costa, L., Henrique, D. and Rossant, J. (2004). Dosage-sensitive requirement for mouse Dll4 in artery development. *Genes Dev.* **18**, 2474-2478.

Fischer, A., Schumacher, N., Maier, M., Sendtner, M. and Gessler, M. (2004). The Notch target genes Hey1 and Hey2 are required for embryonic vascular development. *Genes Dev.* **18**, 901-911.

Gale, N. W., Dominguez, M. G., Noguera, I., Pan, L., Hughes, V., Valenzuela, D. M., Murphy, A. J., Adams, N. C., Lin, H. C., Holash, J. et al. (2004). Haploinsufficiency of delta-like 4 ligand results in embryonic lethality due to major defects in arterial and vascular development. *Proc. Natl. Acad. Sci. USA* **101**, 15949-15954.

Grandbarbe, L., Bouissac, J., Rand, M., Hrabe de Angelis, M., Artavanis-Tsakonas, S. and Mohier, E. (2003). Delta-Notch signaling controls the generation of neurons/glia from neural stem cells in a stepwise process. *Development* **130**, 1391-1402.

Gray, M., Moens, C. B., Amacher, S. L., Eisen, J. S. and Beattie, C. E. (2001). Zebrafish deadly seven functions in neurogenesis. *Dev. Biol.* **237**, 306-323.

Harper, J. A., Yuan, J. S., Tan, J. B., Visan, I. and Guidos, C. J. (2003). Notch signaling in development and disease. *Clin. Genet.* **64**, 461-472.

Hrabe de Angelis, M., McIntyre, J., 2nd and Gossler, A. (1997). Maintenance of somite borders in mice requires the Delta hoMol.ogue Dll1. *Nature* **386**, 717-721.

Iso, T., Kedes, L. and Hamamori, Y. (2003). HES and HERP families: multiple effectors of the Notch signaling pathway. *J. Cell Physiol.* **194**, 237-255.

Itoh, M., Kim, C. H., Palardy, G., Oda, T., Jiang, Y. J., Maust, D., Yeo, S. Y., Lorick, K., Wright, G. J., Ariza-McNaughton, L. et al. (2003). Mind bomb is a ubiquitin ligase that is essential for efficient activation of Notch signaling by Delta. *Dev. Cell* **4**, 67-82.

Jiang, R., Lan, Y., Chapman, H. D., Shawber, C., Norton, C. R., Serreze, D. V., Weinmaster, G. and Gridley, T. (1998). Defects in limb, craniofacial, and thymic development in Jagged2 mutant mice. *Genes Dev.* **12**, 1046-1057.

Jiang, Y. J., Brand, M., Heisenberg, C. P., Beuchle, D., Furutani-Seiki, M., Kelsh, R. N., Warga, R. M., Granato, M., Haffter, P., Hammerschmidt, M. et al. (1996). Mutations affecting neurogenesis and brain morphology in the zebrafish, *Danio rerio*. *Development* **123**, 205-216.

Jiang, Y. J., Aerne, B. L., Smithers, L., Haddon, C., Ish-Horowicz, D. and Lewis, J. (2000). Notch signalling and the synchronization of the somite segmentation clock. *Nature* **408**, 475-479.

Klueg, K. M. and Muskavitch, M. A. (1999). Ligand-receptor interactions and trans-endocytosis of Delta, Serrate and Notch: members of the Notch signalling pathway in Drosophila. *J. Cell Sci.* **112**, 3289-3297.

Koo, B. K., Yoon, K. J., Yoo, K. W., Lim, H. S., Song, R., So, J. H., Kim, C. H. and Kong, Y. Y. (2005). Mind bomb-2 is an E3 ligase for notch ligand. *J. Biol. Chem.* **280**, 22335-22342.

Krebs, L. T., Xue, Y., Norton, C. R., Shutter, J. R., Maguire, M., Sundberg, J. P., Gallahan, D., Closson, V., Kitajewski, J., Callahan, R. et al. (2000). Notch signaling is essential for vascular morphogenesis in mice. *Genes Dev.* **14**, 1343-1352.

Krebs, L. T., Shutter, J. R., Tanigaki, K., Honjo, T., Stark, K. L. and Gridley, T. (2004). Haploinsufficient lethality and formation of arteriovenous malformations in Notch pathway mutants. *Genes Dev.* **18**, 2469-2473.

Kusumi, K., Sun, E. S., Kerrebrock, A. W., Bronson, R. T., Chi, D. C., Bulotsky, M. S., Spencer, J. B., Birren, B. W., Frankel, W. N. and Lander, E. S. (1998). The mouse pudgy mutation disrupts Delta hoMol.ogue Dll3 and initiation of early somite boundaries. *Nat. Genet.* **19**, 274-278.

Lai, E. C. (2004). Notch signaling: control of cell communication and cell fate. *Development* **131**, 965-973.

Lai, E. C., Deblandre, G. A., Kintner, C. and Rubin, G. M. (2001). Drosophila neuralized is a ubiquitin ligase that promotes the internalization and degradation of delta. *Dev. Cell* **1**, 783-794.

Lai, E. C., Roegiers, F., Qin, X., Jan, Y. N. and Rubin, G. M. (2005). The ubiquitin ligase Drosophila Mind bomb promotes Notch signaling by regulating the localization and activity of Serrate and Delta. *Development* **132**, 2319-2332.

Lawson, N. D., Scheer, N., Pham, V. N., Kim, C. H., Chitnis, A. B., Campos-Ortega, J. A. and Weinstein, B. M. (2001). Notch signaling is required for arterial-venous differentiation during embryonic vascular development. *Development* **128**, 3675-3683.

Le Borgne, R. and Schweisguth, F. (2003). Notch signaling: endocytosis makes delta signal better. *Curr. Biol.* **13**, R273-R275.

Le Borgne, R., Remaud, S., Hamel, S. and Schweisguth, F. (2005). Two distinct E3 ubiquitin ligases have complementary functions in the regulation of delta and serrate signaling in Drosophila. *PLoS Biol.* **3**, e96.

Leitges, M., Neidhardt, L., Haenig, B., Herrmann, B. G. and Kispert, A. (2000). The paired homeobox gene Uncx4.1 specifies pedicles, transverse processes and proximal ribs of the vertebral column. *Development* **127**, 2259-2267.

Ma, Q., Chen, Z., del Barco Barrantes, I., de la Pompa, J. L. and Anderson, D. J. (1998). neurogenin1 is essential for the determination of neuronal precursors for proximal cranial sensory ganglia. *Neuron* **20**, 469-482.

Mumm, J. S., Schroeter, E. H., Saxena, M. T., Griesemer, A., Tian, X., Pan, D. J., Ray, W. J. and Kopan, R. (2000). A ligand-induced extracellular cleavage regulates gamma-secretase-like proteolytic activation of Notch1. *Mol. Cell* **5**, 197-206.

Ohtsuka, T., Ishibashi, M., Gradwohl, G., Nakanishi, S., Guillemot, F. and Kageyama, R. (1999). Hes1 and Hes5 as notch effectors in mammalian neuronal differentiation. *EMBO J.* **18**, 2196-2207.

Oka, C., Nakano, T., Wakeham, A., de la Pompa, J. L., Mori, C., Sakai, T., Okazaki, S., Kawaichi, M., Shiota, K., Mak, T. W. et al. (1995). Disruption of the mouse RBP-J kappa gene results in early embryonic death. *Development* **121**, 3291-3301.

Parks, A. L., Klueg, K. M., Stout, J. R. and Muskavitch, M. A. (2000). Ligand endocytosis drives receptor dissociation and activation in the Notch pathway. *Development* **127**, 1373-1385.

Pavlopoulos, E., Pitsouli, C., Klueg, K. M., Muskavitch, M. A., Moschonas, N. K. and Delidakis, C. (2001). neuralized Encodes a peripheral membrane protein involved in delta signaling and endocytosis. *Dev. Cell* **1**, 807-816.

Price, B. D., Chang, Z., Smith, R., Bockheim, S. and Laughon, A. (1993). The Drosophila neuralized gene encodes a C3HC4 zinc finger. *EMBO J.* **12**, 2411-2418.

Radtke, F., Wilson, A., Ernst, B. and MacDonald, H. R. (2002). The role of Notch signaling during hematopoietic lineage commitment. *Immunol. Rev.* **187**, 65-74.

Riley, B. B., Chiang, M., Farmer, L. and Heck, R. (1999). The deltaA gene of zebrafish mediates lateral inhibition of hair cells in the inner ear and is regulated by pax2.1. *Development* **126**, 5669-5678.

Ross, S. E., Greenberg, M. E. and Stiles, C. D. (2003). Basic helix-loop-helix factors in cortical development. *Neuron* **39**, 13-25.

Ruan, Y., Tecott, L., Jiang, M. M., Jan, L. Y. and Jan, Y. N. (2001). Ethanol hypersensitivity and olfactory discrimination defect in mice lacking a hoMol.og of Drosophila neuralized. *Proc. Natl. Acad. Sci. USA* **98**, 9907-9912.

Schier, A. F., Neuhauss, S. C., Harvey, M., Malicki, J., Solnica-Krezel, L., Stainier, D. Y., Zwartkruis, F., Abdelilah, S., Stemple, D. L., Rangini, Z. et al. (1996). Mutations affecting the development of the embryonic zebrafish brain. *Development* **123**, 165-178.

Schweisguth, F. (2004). Notch signaling activity. *Curr. Biol.* **14**, R129-R138.

Shi, S. and Stanley, P. (2003). Protein O-fucosyltransferase 1 is an essential component of Notch signaling pathways. *Proc. Natl. Acad. Sci. USA* **100**, 5234-5239.

Vollrath, B., Pudney, J., Asa, S., Leder, P. and Fitzgerald, K. (2001). Isolation of a murine hoMol.ogue of the Drosophila neuralized gene, a gene required for axonemal integrity in spermatozoa and terminal maturation of the mammary gland. *Mol. Cell Biol.* **21**, 7481-7494.

Xue, Y., Gao, X., Lindsell, C. E., Norton, C. R., Chang, B., Hicks, C., Gendron-Maguire, M., Rand, E. B., Weinmaster, G. and Gridley, T. (1999). Embryonic lethality and vascular defects in mice lacking the Notch ligand Jagged1. *Hum. Mol. Genet.* **8**, 723-730.

Table S1. Genotypes of embryos and mice from *mib*$^{+/-}$ intercrosses

Stage	Number of embryos or mice (%)			Total
	+/+	+/–	–/–	
9.5 dpc	24 (29.3)	38 (46.3)	20 (24.4)	82
10.5 dpc	10 (24.4)	24 (58.5)	7 (17.1)	41
11.5 dpc	16 (34.0)	31 (66.0)	0	47
12.5 dpc	7 (33.3)	14 (66.7)	0	21
3 weeks	19 (35.8)	34 (64.2)	0	53